



Crystal structure and Hirshfeld surface analysis of dibromidobis({(S)-2-[1-(dimethylamino)ethyl]-phenyl}diphenylsilanol-κO)zinc(II)

Julius Hättasch, Franziska Dorothea Klotz, Annika Schmidt and Carsten Strohmann*

Received 5 August 2025
Accepted 15 October 2025

Technische Universität Dortmund, Fakultät für Chemie und Chemische Biologie, Otto-Hahn-Strasse 6, 44227 Dortmund, Germany. *Correspondence e-mail: carsten.strohmann@tu-dortmund.de

Edited by K. V. Domasevitch, National Taras Shevchenko University of Kyiv, Ukraine

Keywords: crystal structure; zinc bromide complex; chiral silanol ligand; Hirshfeld surface analysis; zwitterionic structure; crystal voids.

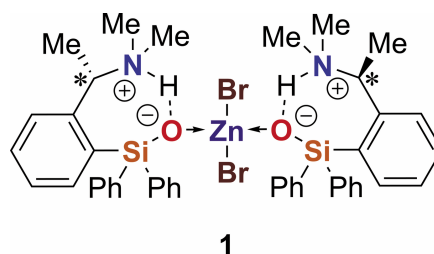
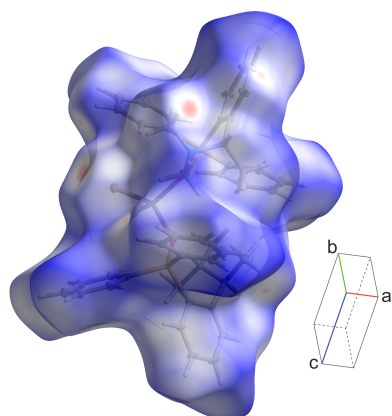
CCDC reference: 2495680

Supporting information: this article has supporting information at journals.iucr.org/e

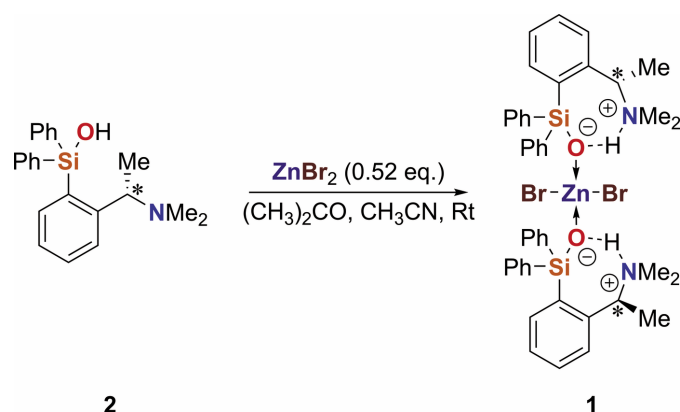
Molecules of the title compound, $[\text{ZnBr}_2(\text{C}_{22}\text{H}_{25}\text{NOSi})_2]$, are situated across a twofold axis passing through the central Zn atom in the uncommon space group $C22_1$. The organic ligands feature migration of Si–OH protons to the amine substituents, while the resulting zwitterions adopt strong charge-assisted intramolecular $\text{N}^+\text{H}\cdots\text{O}^-$ hydrogen bonds [$\text{N}\cdots\text{O} = 2.5895(13) \text{ \AA}$]. They act as monodentate ligands through highly nucleophilic silanolate O atoms, completing a distorted ZnBr_2O_2 tetrahedral environment of the metal ions [$\text{Zn}–\text{O} = 1.9509(9) \text{ \AA}$]. In the crystal, weak $\text{C}–\text{H}\cdots\text{Br}$ hydrogen bonds govern the assembly of a two-dimensional pattern parallel to the (110) plane, further consolidated by $\text{C}–\text{H}\cdots\pi$ bonding. These findings are in line with the results of Hirshfeld surface analysis. The latter reveals the prevalence of $\text{H}\cdots\text{H}$ interactions (67.9%), which are followed by $\text{H}\cdots\text{C}/\text{C}\cdots\text{H}$ (21.5%) and $\text{Br}\cdots\text{H}/\text{H}\cdots\text{Br}$ (10.5%) contacts. The fingerprint plots also indicate the presence of crystal voids that are consistent with a relatively loose packing.

1. Chemical context

Silanols are a versatile class of compounds that are used both in the chemical industry and in organic synthesis. Their importance ranges from their use as column materials, for example, in the form of silica gel (Ritgen, 2019), to their role as reactants in coupling reactions (Hirabayashi *et al.*, 1998). In addition, silanol functionalities have been employed as bioisosteres for hydroxyl groups in drug development, both by modifying known compounds and by designing new silanol-based molecules. Several of these derivatives have shown promising biological properties (Showell *et al.*, 2006; Tacke *et al.*, 1989, 1991). Silanols can also be used as temporary ligands to control the regioselectivity of metal-catalyzed reactions (Yamagishi *et al.*, 2023). Furthermore, zinc siloxides can act as protected forms of silanols, bypassing the often poor stability of silanols towards condensation (Golz *et al.*, 2017). The work presented here shows a stable and carbon-chiral silanol molecule (**1**), which can be used for the synthesis of transition-metal complexes.



In the present work, we report on the tetrahedral zinc bromide complex dibromidobis(*(S)*-2-[1-(dimethylamino)ethyl]phenyl)diphenylsilanol- κ O)zinc(II), ZnBr_2L_2 (**1**), adopted by the enantiomerically pure *(S)*-2-[1-(dimethylamino)ethyl]phenyl)diphenylsilanol (**2**) and how the desired silanolate structure ($\text{Si}-\text{O}^-$) may be generated by intramolecular prototropic migration involving silanol ($\text{Si}-\text{OH}$ group) and the tertiary amino groups (Scheme 2). The highly nucleophilic silanolate O-donor sites are prone to coordination to the Lewis acid Zn^{2+} , while retaining markedly strong interaction with the H atoms, which are now located at the adjacent N-atom sites.



2. Structural commentary

The title complex, **1**, crystallizes at room temperature from acetonitrile solution as a molecular complex (Fig. 1 and Table 1). The asymmetric part of the structure comprises one half of a molecule situated across a twofold axis passing through the Zn1 atom. All bond lengths and angles are within the expected ranges as found in the Cambridge Structural

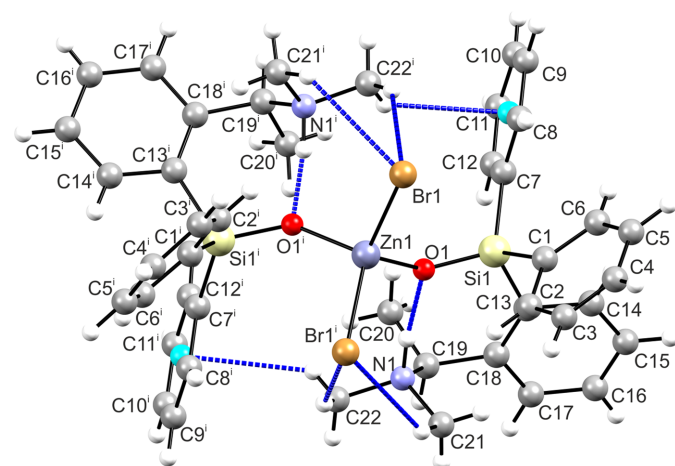


Figure 1
Molecular structure of **1**, drawn with 50% probability displacement ellipsoids, showing intramolecular interactions (dashed blue lines). Relevant ring centroids are represented by light-blue spheres. [Symmetry code: (i) $x, -y + 1, -z + 1$.]

Table 1
Selected geometrical parameters (\AA , $^\circ$) for **1**.

Zn1—O1	1.9509 (9)	Si1—C1	1.8802 (13)
Zn1—Br1	2.39687 (17)	Si1—C7	1.8820 (13)
Si1—O1	1.6135 (9)	Si1—C13	1.8996 (13)
Br1—Zn1—Br1 ⁱ	114.035 (11)	O1 ⁱ —Zn1—O1	102.34 (6)
O1—Zn1—Br1	108.75 (3)	Si1—O1—Zn1	137.64 (5)
O1 ⁱ —Zn1—Br1 ⁱ	111.18 (3)		

Symmetry code: (i) $x, -y + 1, -z + 1$.

Table 2
Hydrogen-bond geometry (\AA , $^\circ$) for **1** compared with other hydrogen-bond geometries.

	$D-H\cdots A$	$D-H$	$H\cdots A$	$D\cdots A$	$D-H\cdots A$
1	N1—H1 \cdots O1	0.95 (2)	1.65 (2)	2.5895 (13)	172 (2)
(Langenohl, 2021)	O1—H1 \cdots N1	0.840 (2)	1.795 (2)	2.628 (2)	171.48 (11)
	O2—H2 \cdots N2	0.840 (2)	1.816 (2)	2.637 (2)	165.20 (11)
BAYVAB	N6—H6 \cdots O4	0.89 (8)	1.77 (7)	2.634 (7)	163 (7)
	N4—H4 \cdots O1	0.99 (10)	1.68 (11)	2.637 (10)	163 (7)
KANNUK	N2—H2 \cdots O3	0.90 (1)	1.82 (5)	2.718 (8)	169 (7)
	N7—H7 \cdots O7	0.90 (1)	1.84 (3)	2.716 (8)	163 (9)

Note: Bond lengths and angles involving H atoms in the literature structures should be interpreted with care, since the H-atom positions were geometrically constrained during refinement. In contrast, all H atoms in the present structure were refined freely.

Database (CSD; Groom *et al.*, 2016; WebCSD September 2025). The zinc ion adopts a slightly distorted tetrahedral coordination geometry, with the largest angle at the central atom sustained with the two bromide ligands [114.035 (11) $^\circ$] and the smallest angle with the two silanolate O atoms [102.34 (6) $^\circ$]. The absolute configuration at the stereogenic centre was confirmed as *S* by X-ray diffraction. The refined Flack x parameter of -0.0041 (15) supports the assignment and matches the configuration of the chiral precursor.

The organic ligand exists in a conformation that is favourable for intramolecular hydrogen bonding involving the precisely positioned silanol and amino groups. Previous X-ray structure studies revealed similar geometry for the non-coordinated species, with the H atom located at the O atom of the silanol group (Langenohl, 2021). In the present case, the coordination to the zinc ion enhances the acidity of the silanol group and promotes the proton transfer to the amine group, thus generating a zwitterionic species in the crystal structure of the complex. With this proton transfer, the charge-assisted intramolecular $\text{N}^+-\text{H}\cdots\text{O}^-$ hydrogen bond actualizes over the neutral reverse pattern $\text{O}-\text{H}\cdots\text{N}$ seen in the non-coordinated precursor **2**. Table 2 compares the observed hydrogen-bond geometries in **1** with those in **2** (Langenohl, 2021) and two related structures from the CSD. The crystals reported by Robert and co-workers (refcode BAYVAB; Nguyen *et al.*, 2017) and by Wang (KANNUK; Wang, 2011) feature the best comparable intermolecular $\text{N}^+-\text{H}\cdots\text{O}^- \cdots \text{Zn}$ motif. Within this comparison, the present hydrogen bond appears to be the strongest, with the shortest donor–acceptor distance and the hydrogen-bond angle nearest to 180° .

The molecular structure of the complex is additionally consolidated by a set of weaker interactions, which include symmetry-related pairs of two $\text{C}-\text{H}\cdots\text{Br}$ bonds [$\text{C}\cdots\text{Br} = 3.7373$ (14) and 3.8552 (14) \AA] and $\text{C}-\text{H}\cdots\pi$ bonds with

Table 3
Hydrogen-bond geometry (Å, °).

<i>D</i> —H··· <i>A</i>	<i>D</i> —H	H··· <i>A</i>	<i>D</i> ··· <i>A</i>	<i>D</i> —H··· <i>A</i>
C21—H21A···Br1 ⁱ	0.96 (2)	3.10 (2)	3.8552 (14)	137.0 (18)
C22—H22A···Br1 ⁱ	0.94 (2)	2.95 (2)	3.7373 (14)	142.1 (17)
C19—H19···Br1 ⁱⁱ	0.92 (2)	3.09 (2)	3.8944 (11)	146.9 (17)
C21—H21C···Br1 ⁱⁱⁱ	0.95 (3)	2.86 (3)	3.7615 (14)	159 (2)
C22—H22B···Cg(C7—C12) ⁱ	0.90 (2)	2.84 (2)	3.4972 (15)	131 (2)
C15—H15···Cg(C1—C6) ⁱⁱⁱ	0.97 (2)	3.11 (2)	3.7553 (16)	125 (2)

Symmetry codes: (i) $x, -y + 1, -z + 1$; (ii) $x + \frac{1}{2}, y - \frac{1}{2}, z$; (iii) $-x + 1, y, -z + \frac{3}{2}$. Cg is the group centroid.

methyl donors (Table 3). Also, one can identify a tetrel bond between Br1 and Si1. It is characterized by a Br1···Si1 distance of 4.1850 (6) Å and a Br1···Si1—C13 angle of 163.03 (4)°. This interaction is likely responsible for the elongation of the Si1—C13 bond by 0.018 (3) Å with respect to the other two Si—C bonds (see Table 1).

3. Supramolecular features

Being dominated rather by dispersion forces, the crystal packing is relatively loose, with a packing index of 67.9. Few identified intermolecular interactions are represented by very weak hydrogen bonding (Table 3). The molecules are linked by double hydrogen bonds C19—H···Br1ⁱⁱ and C21—H···Br1ⁱⁱ [symmetry code: (ii) $x + \frac{1}{2}, y - \frac{1}{2}, z$], which produces a

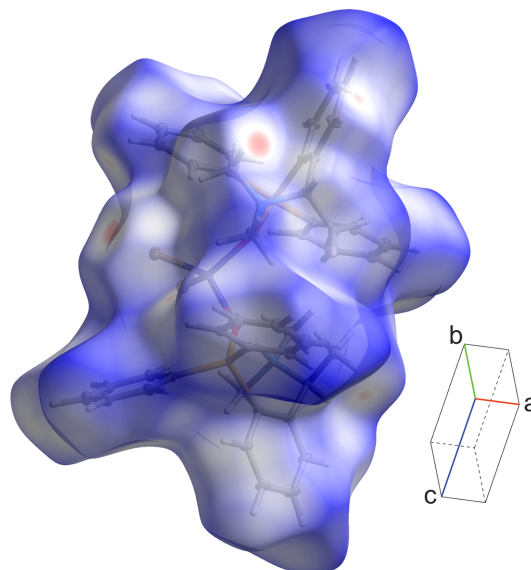


Figure 3
Three-dimensional Hirshfeld surface analysis of **1** mapped over d_{norm} . The red regions correspond to specific intermolecular contacts.

two-dimensional network parallel to (110) (Fig. 2). These layers face each other with phenyl groups and are linked by mutual C—H··· π bonds, namely, C15—H···Cg(C1—C6)ⁱⁱⁱ [Cg is the group centroid; symmetry code: (iii) $-x + 1, y, -z + \frac{3}{2}$]. One can note that beyond the above strongest intramolecular hydrogen bond, five out of six C—H···Br and C—H··· π

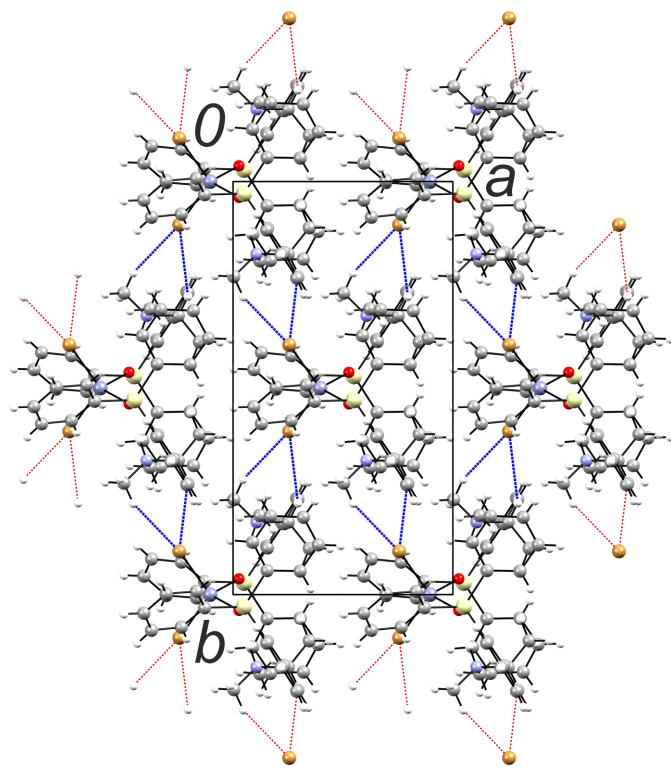


Figure 2
The molecular packing of **1**, viewed along [001], with the unit cell shown as a black outline. The most significant intermolecular interactions within the layer are represented by C—H···Br hydrogen bonds (blue dashed lines).

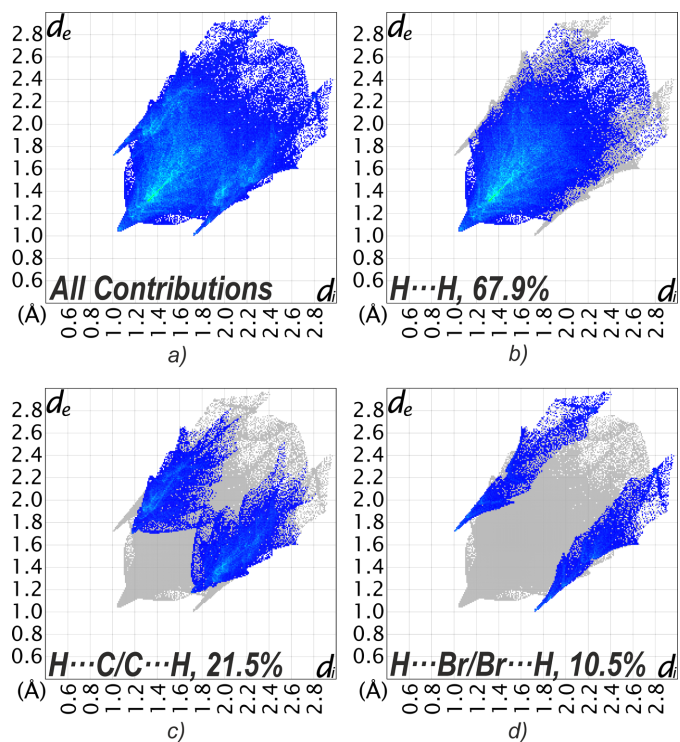


Figure 4
Two-dimensional fingerprint plots for **1**, showing (a) all and (b)–(d) selected interactions in the crystal. d_e and d_i represent the distances from a point on the Hirshfeld surface to the nearest external or internal atom, respectively.

interactions are generated with aliphatic C—H donors in the α -position relative to the N—H⁺ site.

In order to better understand the intermolecular interactions, a Hirshfeld surface analysis was carried out. The Hirshfeld surface and fingerprint plots (McKinnon *et al.*, 2007) were created using *CrystalExplorer21* (Spackman *et al.*, 2021). The Hirshfeld surface shown in Fig. 3 was mapped over d_{norm} in the range from -0.143 to 1.476 a.u. It highlights 12 close contacts as red spots, whereas blue regions indicate intermolecular separations above the sum of the atomic radii. The most intense spots correspond to the Br \cdots H/H \cdots Br interactions described above, although even in such cases the contacts approach the normal van der Waals (vdW) separations. Each of the two silanolate ligands contributes six contacts, which complete the molecular environments in the layers parallel to the (110) plane.

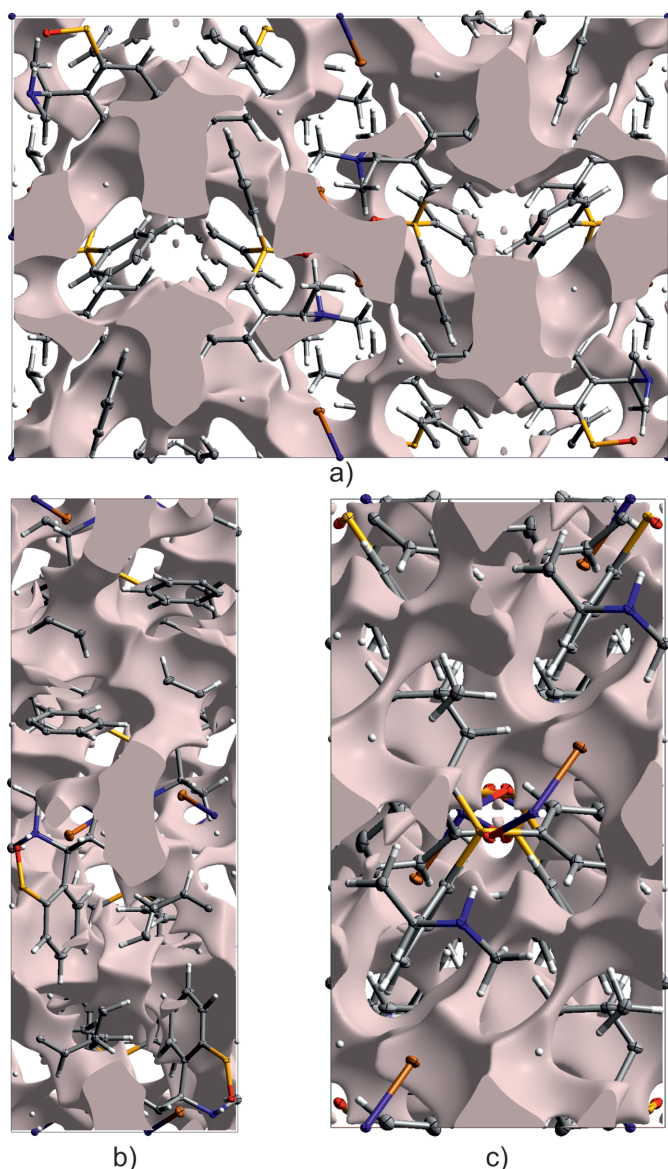


Figure 5
Views of the calculated *Crystal Voids* isosurface in the (a) [100], (b) [010] and (c) [001] direction.

The relative contributions of the intermolecular interactions in compound **1** were also analyzed using two-dimensional fingerprint plots (Spackman & McKinnon, 2002). As expected, H \cdots H contacts are the most significant, accounting for 67.9% of the surface (Fig. 4), reflecting the importance of vdW interactions to the packing. H \cdots C/C \cdots H contacts contribute 21.5%, which is consistent with the presence of weak C—H \cdots π interactions or general hydrophobic contacts involving the phenyl substituents. The Br \cdots H/H \cdots Br interactions account for 10.5% of the surface area and represent the main directional contacts in the supramolecular structure. There are no C \cdots C contacts, in accordance with the absence of significant π – π interactions. The fingerprint plots also show a diffuse collection of points above d_e , $d_i = 2.5$ Å, indicating voids in the crystal structure. This was further investigated by calculating the *Crystal Voids* isosurface (Turner *et al.*, 2011) in *CrystalExplorer21* for the whole unit cell with the isovalue set to 0.002 e a.u.⁻³. The calculated surface with the rescale surface property set to -0.005 to 0.000 is depicted in Fig. 5. For the calculation of the void volume, capping faces are generated on the boundary of the unit cell. With 13.3% (561 Å³) of the volume outside of the isosurface, the crystal of **1** appears packed loose.

4. Database survey

A search of the Cambridge Structural Database (Groom *et al.*, 2016; WebCSD July 2025) for zinc bromide complexes coordinated by siloxy groups revealed several structures, four of which contained bridged Zn—O bonds in which one O atom coordinates to two zinc centres. They are tetrabromodizinc(II) complexes involving μ_2 -1-[[oxy](diphenyl)silyl]methyl]piperidinium, μ_2 -1-[[oxy(dimethyl)silyl]methyl]-5-methylpyrrolidin-1-ium and μ_2 -1-[[oxy(dimethyl)silyl]methyl]-2,6-dimethylpiperidinium (CSD refcodes VUPFAO, VUPFES and VUPFIW, respectively; Däschlein & Strohmam, 2009), as well as bis[μ_2 -1-[[hydroxy(dimethyl)silyl]methyl]piperidiniumato]]tetrabromodizinc(II) (WUDPAN; Däschlein *et al.*, 2009). A closely related structure differs only by the replacement of one phenyl group with a methyl group. The structure of dibromobis[2-[1-(dimethylamino)ethyl]phenyl](methyl)phenylsilanol]zinc(II) acetone solvate (IFUSEL; Langenohl *et al.*, 2023) shows a tetrahedrally coordinated zinc centre, which accommodates two silanolate O ligands. In this complex, the proton is also transferred from the silanol group to the amino group, resulting in a zwitterionic species, as in the present structure. This transfer is also likely induced by an increase in the acidity of the silanol O atom upon coordination to the Zn²⁺ ion.

5. Synthesis and crystallization

The synthesis of the carbon-chiral precursor {(S)-2-[1-(dimethylamino)ethyl]phenyl}diphenylsilanol (**2**) was conducted according to a previously established procedure (Langenohl, 2021). For the synthesis of the title compound (**1**), **2** (347.53 g mol⁻¹, 60.0 mg, 0.17 mmol, 1.00 equiv.) and zinc bromide (225.19 g mol⁻¹, 20.2 mg, 0.09 mmol, 0.52 equiv.)

were each dissolved in 2 ml acetone. The ligand solution was dripped into the metal bromide solution and the solvent was evaporated slowly at room temperature. The resulting solid was not suitable for single-crystal X-ray diffraction and was therefore dissolved in acetonitrile and the solvent evaporated slowly at room temperature again. After 4 d, the product was obtained as colourless blocks.

6. Refinement

Crystal data, data collection and structure refinement details are summarized in Table 4. All H atoms were located in difference maps and then refined with isotropic displacement parameters.

Funding information

Funding for this research was provided by: Studienstiftung des Deutschen Volkes (scholarship to Franziska Dorothea Klotz and Annika Schmidt); Fonds der Chemischen Industrie (scholarship to Annika Schmidt).

References

Bruker (2016). *APEX2*, *SAINT* and *SADABS*. Bruker AXS Inc., Madison, Wisconsin, USA.

Däschlein, C., Bauer, J. O. & Strohmman, C. (2009). *Angew. Chem. Int. Ed.* **48**, 8074–8077.

Däschlein, C. & Strohmman, C. (2009). *Z. Naturforsch. B* **64**, 1558–1579.

Dolomanov, O. V., Bourhis, L. J., Gildea, R. J., Howard, J. A. K. & Puschmann, H. (2009). *J. Appl. Cryst.* **42**, 339–341.

Golz, C., Steffen, P. & Strohmman, C. (2017). *Angew. Chem. Int. Ed.* **56**, 8295–8298.

Groom, C. R., Bruno, I. J., Lightfoot, M. P. & Ward, S. C. (2016). *Acta Cryst.* **B72**, 171–179.

Hirabayashi, K., Nishihara, Y., Mori, A. & Hiyama, T. (1998). *Tetrahedron Lett.* **39**, 7893–7896.

Langenohl, F. (2021). PhD thesis, TU Dortmund University, Dortmund, Germany.

Langenohl, F., Rösler, J., Zühlke, S., Kirchhoff, J.-L. & Strohmman, C. (2023). *Chem. Eur. J.* **29**, e202202935.

McKinnon, J. J., Jayatilaka, D. & Spackman, M. A. (2007). *Chem. Commun.* pp. 3814.

Nguyen, M., Vendier, L., Stigliani, J.-L., Meunier, B. & Robert, A. (2017). *Eur. J. Inorg. Chem.* **2017**, 600–608.

Parsons, S., Flack, H. D. & Wagner, T. (2013). *Acta Cryst.* **B69**, 249–259.

Ritgen, U. (2019). *Anal. Chem.* pp. 150–172 Berlin, Heidelberg: Springer Spektrum.

Sheldrick, G. M. (2008). *Acta Cryst.* **A64**, 112–122.

Sheldrick, G. M. (2015). *Acta Cryst.* **A71**, 3–8.

Table 4

Experimental details.

Crystal data	
Chemical formula	[ZnBr ₂ (C ₂₂ H ₂₅ NOSi) ₂]
<i>M_r</i>	920.23
Crystal system, space group	Orthorhombic, C22 ₁
Temperature (K)	100
<i>a</i> , <i>b</i> , <i>c</i> (Å)	9.3111 (4), 17.5025 (8), 26.0142 (12)
<i>V</i> (Å ³)	4239.5 (3)
<i>Z</i>	4
Radiation type	Mo <i>K</i> α
<i>μ</i> (mm ⁻¹)	2.56
Crystal size (mm)	0.37 × 0.35 × 0.27
Data collection	
Diffractometer	Bruker D8 VENTURE area detector
Absorption correction	Multi-scan (<i>SADABS</i> ; Bruker, 2016)
<i>T_{min}</i> , <i>T_{max}</i>	0.476, 0.568
No. of measured, independent and observed [<i>I</i> > 2σ(<i>I</i>)] reflections	242533, 10338, 9837
<i>R_{int}</i>	0.058
(sin θ/λ) _{max} (Å ⁻¹)	0.834
Refinement	
<i>R</i> [<i>F</i> ² > 2σ(<i>F</i> ²)], <i>wR</i> (<i>F</i> ²), <i>S</i>	0.018, 0.046, 1.06
No. of reflections	10338
No. of parameters	340
H-atom treatment	All H-atom parameters refined
Δρ _{max} , Δρ _{min} (e Å ⁻³)	0.39, -0.35
Absolute structure	Flack <i>x</i> determined using 4306 quotients [(<i>I</i> ⁺ - <i>I</i> ⁻)]/[(<i>I</i> ⁺ + <i>I</i> ⁻)] (Parsons <i>et al.</i> , 2013)
Absolute structure parameter	-0.0041 (15)

Computer programs: *SAINT* (Bruker, 2016), *SHELXT* (Sheldrick, 2015), *SHELXL* (Sheldrick, 2008) and *OLEX2* (Dolomanov *et al.*, 2009).

Showell, G. A., Barnes, M. J., Daiss, J. O., Mills, J. S., Montana, J. G., Tacke, R. & Warneck, J. B. H. (2006). *Bioorg. Med. Chem. Lett.* **16**, 2555–2558.

Spackman, M. A. & McKinnon, J. J. (2002). *CrystEngComm* **4**, 378–392.

Spackman, P. R., Turner, M. J., McKinnon, J. J., Wolff, S. K., Grimwood, D. J., Jayatilaka, D. & Spackman, M. A. (2021). *J. Appl. Cryst.* **54**, 1006–1011.

Tacke, R., Mahner, K., Strohmman, C., Forth, B., Mutschler, E., Friebe, T. & Lambrecht, G. (1991). *J. Organomet. Chem.* **417**, 339–353.

Tacke, R., Rafeiner, K., Strohmman, C., Mutschler, E. & Lambrecht, G. (1989). *Appl. Organomet. Chem.* **3**, 129–132.

Turner, M. J., McKinnon, J. J., Jayatilaka, D. & Spackman, M. A. (2011). *CrystEngComm* **13**, 1804–1813.

Wang, C.-Y. (2011). *Synth. React. Inorg. Met.-Org. Nano-Met. Chem.* **41**, 731–735.

Yamagishi, H., Shimokawa, J. & Yorimitsu, H. (2023). *ACS Catal.* **13**, 7472–7487.

supporting information

Acta Cryst. (2025). E81, 1050-1054 [https://doi.org/10.1107/S2056989025008989]

Crystal structure and Hirshfeld surface analysis of dibromidobis({(S)-2-[1-(dimethylamino)ethyl]phenyl}diphenylsilanol- κ O)zinc(II)

Julius Hättasch, Franziska Dorothea Klotz, Annika Schmidt and Carsten Strohmann

Computing details

Dibromidobis({(S)-2-[1-(dimethylamino)ethyl]phenyl}diphenylsilanol- κ O)zinc(II)

Crystal data

[ZnBr₂(C₂₂H₂₅NOSi)₂]

$M_r = 920.23$

Orthorhombic, C222₁

$a = 9.3111$ (4) Å

$b = 17.5025$ (8) Å

$c = 26.0142$ (12) Å

$V = 4239.5$ (3) Å³

$Z = 4$

$F(000) = 1888$

$D_x = 1.442$ Mg m⁻³

Mo $K\alpha$ radiation, $\lambda = 0.71073$ Å

Cell parameters from 9405 reflections

$\theta = 2.5$ – 35.9°

$\mu = 2.56$ mm⁻¹

$T = 100$ K

Block, colourless

$0.37 \times 0.35 \times 0.27$ mm

Data collection

Bruker D8 VENTURE area detector
diffractometer

Radiation source: microfocus sealed X-ray tube,
Incoatec I μ s

HELIOS mirror optics monochromator

Detector resolution: 10.4167 pixels mm⁻¹

ω and φ scans

Absorption correction: multi-scan
(SADABS; Bruker, 2016)

$T_{\min} = 0.476$, $T_{\max} = 0.568$

242533 measured reflections

10338 independent reflections

9837 reflections with $I > 2\sigma(I)$

$R_{\text{int}} = 0.058$

$\theta_{\max} = 36.4^\circ$, $\theta_{\min} = 2.3^\circ$

$h = -15 \rightarrow 15$

$k = -29 \rightarrow 29$

$l = -43 \rightarrow 43$

Refinement

Refinement on F^2

Least-squares matrix: full

$R[F^2 > 2\sigma(F^2)] = 0.018$

$wR(F^2) = 0.046$

$S = 1.06$

10338 reflections

340 parameters

0 restraints

Primary atom site location: dual

Hydrogen site location: difference Fourier map

All H-atom parameters refined

$w = 1/[\sigma^2(F_o^2) + (0.0262P)^2 + 0.5577P]$

where $P = (F_o^2 + 2F_c^2)/3$

$(\Delta/\sigma)_{\max} = 0.003$

$\Delta\rho_{\max} = 0.39$ e Å⁻³

$\Delta\rho_{\min} = -0.35$ e Å⁻³

Absolute structure: Flack x determined using

4306 quotients [(I+)-(I-)]/[(I+)+(I-)] (Parsons *et al.*, 2013)

Absolute structure parameter: -0.0041 (15)

Special details

Geometry. All esds (except the esd in the dihedral angle between two l.s. planes) are estimated using the full covariance matrix. The cell esds are taken into account individually in the estimation of esds in distances, angles and torsion angles; correlations between esds in cell parameters are only used when they are defined by crystal symmetry. An approximate (isotropic) treatment of cell esds is used for estimating esds involving l.s. planes.

Fractional atomic coordinates and isotropic or equivalent isotropic displacement parameters (\AA^2)

	<i>x</i>	<i>y</i>	<i>z</i>	$U_{\text{iso}}^*/U_{\text{eq}}$
Br1	0.25556 (2)	0.60464 (2)	0.53188 (2)	0.01751 (3)
Zn1	0.39569 (2)	0.500000	0.500000	0.00923 (3)
Si1	0.55007 (4)	0.47098 (2)	0.61362 (2)	0.01029 (5)
O1	0.52706 (10)	0.46179 (5)	0.55246 (3)	0.01189 (14)
N1	0.60742 (12)	0.32472 (6)	0.52845 (4)	0.01226 (16)
H1	0.575 (3)	0.3754 (13)	0.5341 (9)	0.022 (5)*
C1	0.37053 (13)	0.46827 (8)	0.64665 (5)	0.01371 (19)
C2	0.26485 (15)	0.42116 (8)	0.62474 (5)	0.0176 (2)
H2	0.289 (3)	0.3938 (14)	0.5950 (9)	0.025 (6)*
C3	0.12921 (16)	0.41381 (11)	0.64674 (6)	0.0234 (3)
H3	0.065 (3)	0.3821 (15)	0.6304 (10)	0.032 (6)*
C4	0.09460 (17)	0.45510 (11)	0.69067 (6)	0.0261 (3)
H4	0.003 (3)	0.4532 (16)	0.7029 (10)	0.036 (7)*
C5	0.19603 (17)	0.50221 (11)	0.71296 (5)	0.0247 (3)
H5	0.170 (3)	0.5321 (16)	0.7450 (10)	0.040 (7)*
C6	0.33367 (16)	0.50790 (9)	0.69169 (5)	0.0185 (2)
H6	0.405 (3)	0.5389 (14)	0.7069 (9)	0.025 (6)*
C7	0.65495 (14)	0.55833 (7)	0.63287 (5)	0.01323 (19)
C8	0.58967 (16)	0.62692 (7)	0.64829 (5)	0.0163 (2)
H8	0.488 (3)	0.6317 (14)	0.6486 (9)	0.024 (6)*
C9	0.67035 (19)	0.69061 (8)	0.66218 (6)	0.0203 (3)
H9	0.622 (3)	0.7365 (16)	0.6725 (11)	0.030 (6)*
C10	0.81991 (19)	0.68746 (9)	0.66063 (6)	0.0226 (3)
H10	0.873 (3)	0.7272 (16)	0.6686 (10)	0.029 (6)*
C11	0.88751 (18)	0.62054 (9)	0.64493 (6)	0.0226 (3)
H11	0.989 (3)	0.6187 (15)	0.6434 (9)	0.027 (6)*
C12	0.80564 (15)	0.55698 (8)	0.63162 (6)	0.0176 (2)
H12	0.852 (2)	0.5143 (14)	0.6239 (9)	0.024 (6)*
C13	0.65665 (13)	0.38691 (7)	0.63965 (4)	0.01183 (18)
C14	0.65333 (16)	0.38275 (8)	0.69366 (5)	0.0163 (2)
H14	0.608 (3)	0.4211 (13)	0.7111 (8)	0.019 (5)*
C15	0.71940 (18)	0.32442 (9)	0.72139 (5)	0.0209 (3)
H15	0.717 (2)	0.3224 (12)	0.7586 (8)	0.020 (5)*
C16	0.78960 (19)	0.26659 (9)	0.69506 (6)	0.0233 (3)
H16	0.821 (3)	0.2275 (16)	0.7113 (10)	0.033 (7)*
C17	0.79479 (17)	0.26874 (8)	0.64160 (5)	0.0195 (2)
H17	0.842 (3)	0.2269 (15)	0.6232 (10)	0.028 (6)*
C18	0.73154 (13)	0.32825 (7)	0.61381 (4)	0.01269 (18)
C19	0.75106 (15)	0.32433 (6)	0.55560 (4)	0.01300 (17)

H19	0.795 (2)	0.2781 (13)	0.5488 (8)	0.019 (5)*
C20	0.84696 (14)	0.38824 (8)	0.53486 (5)	0.0171 (2)
H20A	0.939 (3)	0.3884 (15)	0.5554 (10)	0.029 (6)*
H20B	0.808 (2)	0.4402 (13)	0.5386 (8)	0.019 (5)*
H20C	0.872 (3)	0.3816 (15)	0.5020 (11)	0.034 (6)*
C21	0.50345 (15)	0.26999 (8)	0.55163 (5)	0.0162 (2)
H21A	0.418 (3)	0.2724 (14)	0.5309 (9)	0.024 (6)*
H21B	0.485 (3)	0.2802 (13)	0.5849 (9)	0.021 (5)*
H21C	0.546 (3)	0.2208 (16)	0.5503 (10)	0.034 (7)*
C22	0.62173 (15)	0.30815 (9)	0.47251 (5)	0.0181 (2)
H22A	0.530 (2)	0.3126 (12)	0.4577 (8)	0.014 (5)*
H22B	0.683 (2)	0.3415 (13)	0.4582 (8)	0.015 (5)*
H22C	0.658 (3)	0.2589 (15)	0.4673 (10)	0.027 (6)*

Atomic displacement parameters (Å²)

	U^{11}	U^{22}	U^{33}	U^{12}	U^{13}	U^{23}
Br1	0.01733 (5)	0.01215 (5)	0.02303 (6)	0.00417 (4)	0.00357 (5)	−0.00182 (4)
Zn1	0.01005 (7)	0.00799 (7)	0.00967 (7)	0.000	0.000	0.00028 (6)
Si1	0.01207 (13)	0.00994 (12)	0.00887 (12)	0.00211 (10)	−0.00017 (10)	−0.00023 (10)
O1	0.0139 (4)	0.0123 (3)	0.0096 (3)	0.0031 (3)	−0.0008 (3)	0.0001 (3)
N1	0.0131 (4)	0.0122 (4)	0.0114 (4)	0.0019 (3)	−0.0006 (3)	−0.0007 (3)
C1	0.0143 (5)	0.0160 (5)	0.0109 (4)	0.0030 (4)	0.0010 (4)	0.0011 (4)
C2	0.0154 (5)	0.0235 (5)	0.0140 (5)	−0.0002 (5)	0.0006 (4)	0.0004 (4)
C3	0.0145 (5)	0.0380 (8)	0.0177 (6)	−0.0018 (5)	−0.0002 (4)	0.0053 (5)
C4	0.0161 (6)	0.0437 (9)	0.0186 (6)	0.0061 (6)	0.0047 (5)	0.0063 (6)
C5	0.0254 (6)	0.0330 (7)	0.0155 (5)	0.0084 (6)	0.0081 (5)	0.0017 (6)
C6	0.0212 (5)	0.0216 (6)	0.0125 (4)	0.0034 (5)	0.0032 (4)	−0.0006 (4)
C7	0.0162 (5)	0.0117 (4)	0.0118 (5)	0.0016 (4)	−0.0012 (4)	−0.0003 (4)
C8	0.0217 (6)	0.0117 (4)	0.0154 (5)	0.0026 (4)	0.0005 (4)	−0.0003 (4)
C9	0.0301 (7)	0.0123 (5)	0.0186 (6)	−0.0015 (5)	0.0018 (5)	−0.0031 (4)
C10	0.0294 (7)	0.0181 (6)	0.0201 (6)	−0.0078 (5)	0.0002 (5)	−0.0028 (5)
C11	0.0206 (6)	0.0209 (6)	0.0264 (7)	−0.0041 (5)	−0.0014 (5)	−0.0021 (5)
C12	0.0171 (5)	0.0154 (5)	0.0204 (6)	0.0004 (4)	−0.0004 (4)	−0.0024 (4)
C13	0.0136 (4)	0.0118 (4)	0.0101 (4)	0.0013 (4)	−0.0013 (3)	0.0008 (3)
C14	0.0217 (6)	0.0160 (5)	0.0113 (4)	0.0044 (4)	−0.0013 (4)	0.0005 (4)
C15	0.0291 (7)	0.0207 (6)	0.0129 (5)	0.0065 (5)	−0.0030 (5)	0.0034 (4)
C16	0.0319 (7)	0.0208 (6)	0.0172 (5)	0.0106 (5)	−0.0042 (5)	0.0048 (5)
C17	0.0249 (6)	0.0163 (5)	0.0172 (5)	0.0086 (5)	−0.0033 (5)	0.0003 (4)
C18	0.0144 (5)	0.0119 (4)	0.0118 (4)	0.0028 (4)	−0.0017 (4)	0.0002 (3)
C19	0.0123 (4)	0.0143 (4)	0.0124 (4)	0.0035 (4)	−0.0007 (4)	−0.0011 (3)
C20	0.0149 (5)	0.0207 (5)	0.0158 (5)	−0.0015 (4)	0.0021 (4)	−0.0013 (4)
C21	0.0158 (5)	0.0141 (5)	0.0187 (5)	−0.0009 (4)	0.0002 (4)	−0.0006 (4)
C22	0.0188 (5)	0.0235 (6)	0.0120 (5)	0.0032 (5)	−0.0007 (4)	−0.0031 (4)

Geometric parameters (Å, °)

Br1—Zn1	2.3969 (2)	C10—H10	0.88 (3)
Zn1—O1 ⁱ	1.9509 (9)	C10—C11	1.391 (2)
Zn1—O1	1.9509 (9)	C11—H11	0.95 (3)
Si1—O1	1.6135 (9)	C11—C12	1.392 (2)
Si1—C1	1.8802 (13)	C12—H12	0.89 (2)
Si1—C7	1.8819 (13)	C13—C14	1.4074 (17)
Si1—C13	1.8996 (12)	C13—C18	1.4114 (16)
N1—H1	0.95 (2)	C14—H14	0.92 (2)
N1—C19	1.5125 (17)	C14—C15	1.3933 (19)
N1—C21	1.4895 (18)	C15—H15	0.97 (2)
N1—C22	1.4897 (16)	C15—C16	1.386 (2)
C1—C2	1.4046 (19)	C16—H16	0.85 (3)
C1—C6	1.4042 (18)	C16—C17	1.392 (2)
C2—H2	0.94 (2)	C17—H17	0.98 (3)
C2—C3	1.393 (2)	C17—C18	1.3980 (18)
C3—H3	0.92 (3)	C18—C19	1.5267 (16)
C3—C4	1.390 (2)	C19—H19	0.92 (2)
C4—H4	0.92 (3)	C19—C20	1.5296 (19)
C4—C5	1.381 (3)	C20—H20A	1.01 (3)
C5—H5	1.01 (3)	C20—H20B	0.98 (2)
C5—C6	1.400 (2)	C20—H20C	0.89 (3)
C6—H6	0.94 (2)	C21—H21A	0.96 (2)
C7—C8	1.4043 (18)	C21—H21B	0.90 (2)
C7—C12	1.404 (2)	C21—H21C	0.95 (3)
C8—H8	0.95 (3)	C22—H22A	0.94 (2)
C8—C9	1.392 (2)	C22—H22B	0.90 (2)
C9—H9	0.96 (3)	C22—H22C	0.94 (3)
C9—C10	1.394 (2)		
Br1—Zn1—Br1 ⁱ	114.035 (11)	C10—C11—H11	119.5 (16)
O1—Zn1—Br1 ⁱ	108.75 (3)	C10—C11—C12	119.87 (15)
O1 ⁱ —Zn1—Br1	108.75 (3)	C12—C11—H11	120.6 (16)
O1 ⁱ —Zn1—Br1 ⁱ	111.18 (3)	C7—C12—H12	120.5 (15)
O1—Zn1—Br1	111.18 (3)	C11—C12—C7	121.87 (14)
O1 ⁱ —Zn1—O1	102.34 (6)	C11—C12—H12	117.6 (15)
O1—Si1—C1	109.27 (5)	C14—C13—Si1	112.61 (9)
O1—Si1—C7	114.35 (5)	C14—C13—C18	116.66 (11)
O1—Si1—C13	110.10 (5)	C18—C13—Si1	130.68 (9)
C1—Si1—C7	111.12 (6)	C13—C14—H14	117.9 (14)
C1—Si1—C13	106.39 (6)	C15—C14—C13	123.03 (12)
C7—Si1—C13	105.27 (5)	C15—C14—H14	119.1 (14)
Si1—O1—Zn1	137.64 (5)	C14—C15—H15	122.3 (13)
C19—N1—H1	102.5 (14)	C16—C15—C14	119.17 (12)
C21—N1—H1	109.3 (14)	C16—C15—H15	118.5 (13)
C21—N1—C19	112.50 (10)	C15—C16—H16	120.0 (18)
C21—N1—C22	109.17 (11)	C15—C16—C17	119.37 (13)

C22—N1—H1	111.2 (14)	C17—C16—H16	120.3 (18)
C22—N1—C19	112.10 (10)	C16—C17—H17	119.0 (15)
C2—C1—Si1	116.89 (9)	C16—C17—C18	121.48 (13)
C6—C1—Si1	125.89 (10)	C18—C17—H17	119.5 (15)
C6—C1—C2	117.21 (12)	C13—C18—C19	124.32 (10)
C1—C2—H2	117.9 (15)	C17—C18—C13	120.25 (11)
C3—C2—C1	121.52 (13)	C17—C18—C19	115.43 (11)
C3—C2—H2	120.6 (15)	N1—C19—C18	110.97 (10)
C2—C3—H3	117.2 (17)	N1—C19—H19	107.7 (14)
C4—C3—C2	120.01 (15)	N1—C19—C20	110.37 (10)
C4—C3—H3	122.8 (17)	C18—C19—H19	106.3 (14)
C3—C4—H4	119.0 (17)	C18—C19—C20	112.74 (10)
C5—C4—C3	119.80 (14)	C20—C19—H19	108.5 (14)
C5—C4—H4	121.0 (17)	C19—C20—H20A	108.0 (15)
C4—C5—H5	119.1 (16)	C19—C20—H20B	115.2 (13)
C4—C5—C6	120.17 (14)	C19—C20—H20C	113.2 (17)
C6—C5—H5	120.7 (16)	H20A—C20—H20B	104.9 (19)
C1—C6—H6	117.4 (15)	H20A—C20—H20C	107 (2)
C5—C6—C1	121.24 (14)	H20B—C20—H20C	108 (2)
C5—C6—H6	121.4 (14)	N1—C21—H21A	106.4 (15)
C8—C7—Si1	123.09 (10)	N1—C21—H21B	112.8 (15)
C12—C7—Si1	119.93 (10)	N1—C21—H21C	107.4 (17)
C12—C7—C8	116.98 (13)	H21A—C21—H21B	112 (2)
C7—C8—H8	120.6 (15)	H21A—C21—H21C	111 (2)
C9—C8—C7	121.68 (14)	H21B—C21—H21C	107 (2)
C9—C8—H8	117.7 (15)	N1—C22—H22A	107.7 (13)
C8—C9—H9	119.1 (17)	N1—C22—H22B	109.6 (14)
C8—C9—C10	119.99 (15)	N1—C22—H22C	110.8 (16)
C10—C9—H9	120.9 (17)	H22A—C22—H22B	110.8 (18)
C9—C10—H10	121.7 (18)	H22A—C22—H22C	110 (2)
C11—C10—C9	119.59 (15)	H22B—C22—H22C	108 (2)
C11—C10—H10	118.7 (18)		
Si1—C1—C2—C3	178.68 (12)	C7—Si1—C13—C18	-113.32 (12)
Si1—C1—C6—C5	179.58 (12)	C7—C8—C9—C10	0.5 (2)
Si1—C7—C8—C9	-179.84 (11)	C8—C7—C12—C11	-0.1 (2)
Si1—C7—C12—C11	179.22 (12)	C8—C9—C10—C11	0.3 (3)
Si1—C13—C14—C15	177.65 (12)	C9—C10—C11—C12	-0.9 (3)
Si1—C13—C18—C17	-175.57 (11)	C10—C11—C12—C7	0.8 (2)
Si1—C13—C18—C19	4.9 (2)	C12—C7—C8—C9	-0.6 (2)
O1—Si1—C1—C2	33.64 (11)	C13—Si1—O1—Zn1	158.45 (8)
O1—Si1—C1—C6	-147.67 (11)	C13—Si1—C1—C2	-85.19 (11)
O1—Si1—C7—C8	96.35 (12)	C13—Si1—C1—C6	93.50 (12)
O1—Si1—C7—C12	-82.91 (12)	C13—Si1—C7—C8	-142.69 (11)
O1—Si1—C13—C14	-166.90 (10)	C13—Si1—C7—C12	38.05 (13)
O1—Si1—C13—C18	10.39 (14)	C13—C14—C15—C16	-1.3 (2)
C1—Si1—O1—Zn1	41.96 (10)	C13—C18—C19—N1	-57.05 (15)
C1—Si1—C7—C8	-27.92 (13)	C13—C18—C19—C20	67.34 (16)

C1—Si1—C7—C12	152.82 (11)	C14—C13—C18—C17	1.63 (19)
C1—Si1—C13—C14	-48.61 (11)	C14—C13—C18—C19	-177.95 (12)
C1—Si1—C13—C18	128.68 (12)	C14—C15—C16—C17	1.1 (3)
C1—C2—C3—C4	1.6 (2)	C15—C16—C17—C18	0.4 (3)
C2—C1—C6—C5	-1.7 (2)	C16—C17—C18—C13	-1.9 (2)
C2—C3—C4—C5	-1.3 (3)	C16—C17—C18—C19	177.75 (15)
C3—C4—C5—C6	-0.6 (3)	C17—C18—C19—N1	123.36 (12)
C4—C5—C6—C1	2.1 (2)	C17—C18—C19—C20	-112.25 (13)
C6—C1—C2—C3	-0.1 (2)	C18—C13—C14—C15	-0.1 (2)
C7—Si1—O1—Zn1	-83.29 (10)	C21—N1—C19—C18	-47.13 (13)
C7—Si1—C1—C2	160.74 (10)	C21—N1—C19—C20	-172.85 (10)
C7—Si1—C1—C6	-20.57 (13)	C22—N1—C19—C18	-170.62 (10)
C7—Si1—C13—C14	69.39 (11)	C22—N1—C19—C20	63.66 (13)

Symmetry code: (i) $x, -y+1, -z+1$.

Hydrogen-bond geometry ($\text{\AA}, ^\circ$)

$D-H\cdots A$	$D-H$	$H\cdots A$	$D\cdots A$	$D-H\cdots A$
C21—H21A \cdots Br1 ⁱ	0.96 (2)	3.10 (2)	3.8552 (14)	137.0 (18)
C22—H22A \cdots Br1 ⁱ	0.94 (2)	2.95 (2)	3.7373 (14)	142.1 (17)
C19—H19 \cdots Br1 ⁱⁱ	0.92 (2)	3.09 (2)	3.8944 (11)	146.9 (17)
C21—H21C \cdots Br1 ⁱⁱ	0.95 (3)	2.86 (3)	3.7615 (14)	159 (2)
C22—H22B \cdots Cg(C7-12) ⁱ	0.90 (2)	2.84 (2)	3.4972 (15)	131 (2)
C15—H15 \cdots Cg(1-6) ⁱⁱⁱ	0.97 (2)	3.11 (2)	3.7553 (16)	125 (2)

Symmetry codes: (i) $x, -y+1, -z+1$; (ii) $x+1/2, y-1/2, z$; (iii) $-x+1, y, -z+3/2$.